P11.2 THERMODYNAMIC AND KINEMATIC ANALYSIS OF MULTIPLE RFD SURGES FOR THE 24 JUNE 2003 MANCHESTER, SOUTH DAKOTA CYCLIC TORNADIC SUPERCELL DURING PROJECT ANSWERS 2003

Bruce D. Lee and Catherine A. Finley

WindLogics, Inc.
Grand Rapids, Minnesota

Patrick Skinner

WeatherBank, Inc.
Edmond, Oklahoma

1. INTRODUCTION

During Project ANSWERS 2003 (Analysis of the Near-Surface Wind and Environment Along the Rear Flank of Supercells), mobile mesonet data (Straka et al. 1996) was collected on a cyclic tornadic supercell that tracked from near Woonsocket to Bryant, South Dakota on 24 June 2003. A large F4 tornado, one of the many tornadoes associated with this storm, destroyed the town of Manchester. This tornado was one of at least 8 tornadoes observed by the ANSWERS teams on this evening. The ANSWERS mesonet collected a rare observational dataset from within the rear flank downdraft (RFD) surge and along the RFD surge boundary in the early, mature and dissipating stages of the Manchester tornado. At times, the leading part of the mesonet was within 1 – 1.5 km of the tornado. In addition, the mesonets collected data on 3 other surges from this storm as well as 2 additional mature RFDs. As will be discussed in sections 4 and 5, the various RFD surges from the same parent storm exhibited a variety of thermodynamic and kinematic signals. The tornadoes associated with the Manchester storm represented a modest portion of the record 70 tornadoes reported in eastern South Dakota on this evening (*National Climatic Data Center*). This localized tornado outbreak also included 21, 12 and 2 tornadoes in Minnesota, Nebraska and Iowa, respectively.

Project ANSWERS 2003 was conducted to gather and analyze near-surface thermodynamic and kinematic datasets near the RFD boundary (RFDB) and within the RFD of tornadic and non-tornadic supercell thunderstorms. While the analyzed dataset of RFD events sampled by mobile mesonets for tornadic and non-tornadic supercells as presented by Markowski et al. (2002) is significant in size, it is not exhaustive given the latitude of the potential scenarios leading to tornadogenesis or tornadogenesis failure. There is a need for mobile mesonet datasets that capture RFD surge evolution and the RFD evolution in cyclic tornadic supercells. There is also a need for high density mobile mesonet observations near specific boundary structures on the periphery of the tornadogenesis region.

Project ANSWERS 2003 was designed to address a number of hypothesis-driven objectives that involve attributes of the RFD and RFDB environment as they pertain to topics ranging from low-level mesocyclogenesis and tornadogenesis (and maintenance) to gustnado occurrence. The project was carried out from mid-May until late June with a domain that included regions from the upper Midwest through the southern Great Plains. ANSWERS had a typical compliment of 4 mesonets with 3 teams from the University of Northern Colorado and 1 from Texas Tech University. Nowcasting support was provided by participants from the University of Northern Colorado and the University of Illinois.

2. SYNOPTIC/MESOSCALE ENVIRONMENT

The target region for potentially tornadic supercells on 24 June became more focused in southeast and east central South Dakota as the day progressed. The best combination of convective trigger, vertical shear, CAPE and low lifted condensation levels appeared to be along and near the warm front paralleling Interstate 90 by late afternoon. Figure 1 shows the synoptic setup for the day with a surface low near Chamberlain, South Dakota. This surface low accompanied a marked jet streak (85 kt at 200

Corresponding author address: Dr. Bruce D. Lee
WindLogics, Inc. – Itasca Technology Center
Grand Rapids, MN 55744
email: blee@windlogics.com

mb) and associated short wave in the upper levels. Team intercepts were anticipated for convective initiation near the warm front extending east of the low in the 2100 – 2300 UTC time period. The low-level airmass just south of the warm front was warm and moisture laden as illustrated by Mitchell's 2342 UTC ASOS observation of 88 F with a 79 F dew point. Of interest for the project were the mesoscale conditions just north of the warm front for storms initiating near the front and moving north of the warm front with an anticipated motion of 230° at 30 kts.

Obtaining a representative sounding for the environment east of Huron that is appropriate for the pre-storm environment of the Manchester supercell is problematic. The nearest sounding site is located approximately 137 km north at Aberdeen. This KABR sounding, located well north of the warm front, is too cool in the lowest 1 km of the atmosphere. In an effort to arrive at a sounding more representative of the general pre-storm environment just north of the warm front in eastern South Dakota, a sounding was created (Fig. 2) using the KABR 00 UTC data modified with average surface thermodynamic conditions from the 2343 UTC ASOS data at Watertown and Brookings, South Dakota. Both of these sites were north of the warm front and had very similar conditions at 2343 UTC. The surface conditions were linearly blended back into the KABR sounding up to the 850 mb level (the base of warm front inversion) to establish the modified sounding's lowest 1 km layer. The modified sounding lacks low-level CIN; however, by 0000 UTC, based on observations (radar and visual) the convective inhibition in the area was likely small. Since corroborating data from other sites in the vicinity showed east to northeast surface winds similar to KABR surface winds, no adjustments were made to the KABR vertical profile of the horizontal winds. Since the mid-tropospheric temperatures were likely slightly cooler over KABR, the convective forecasting thermodynamic parameters modestly overstate the potential convective instability in the region of interest. Even with this caveat, the CAPE would still be large with the calculated value for this sounding of 4162 J kg^{-1}. Notable on this day were the various vertical shear and shear/CAPE hybrid indices. Storm Relative Helicity (Davies-Jones et al. 1990) for the 0-3 and 0-1 km layers

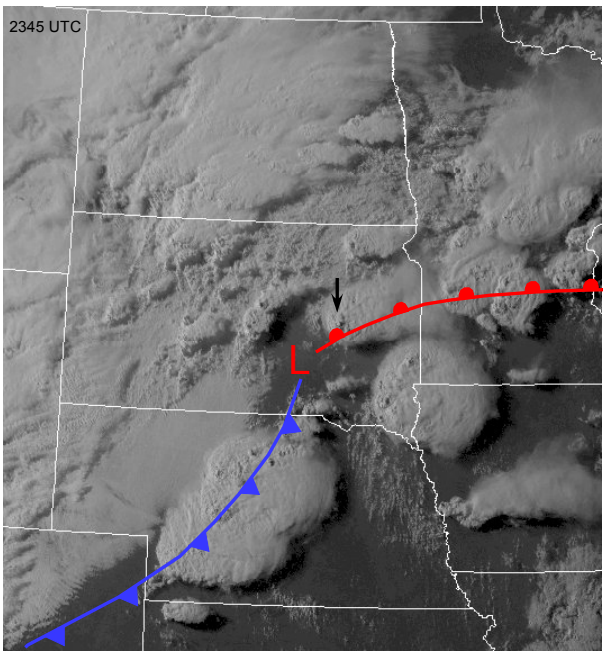

Fig. 1. Synoptic conditions at 2343 UTC on 24 June 2003. Background is GOES 12 visible imagery. Low pressure center and attendant fronts were based on the 2343 UTC regional surface observations. Arrow indicates the Manchester target storm.

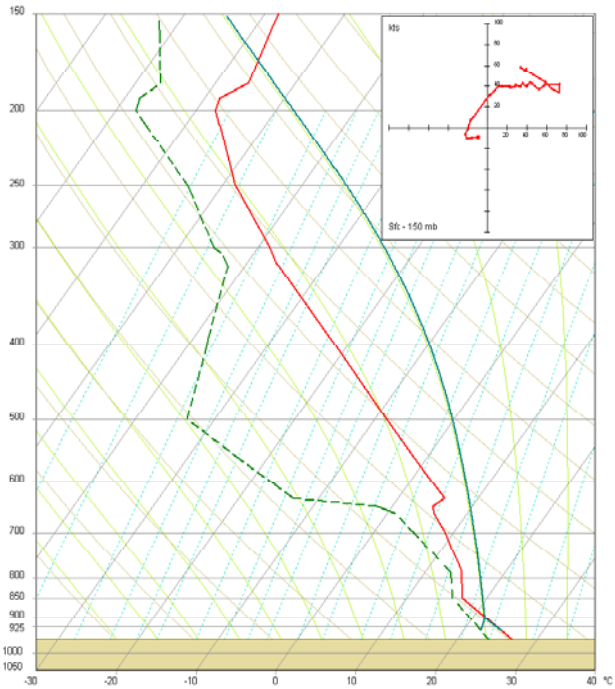

Fig. 2. Modified KABR sounding reflective of the surface thermodynamic character just north of the warm front in Fig. 1. The dark green line represents the parcel accent path employing a 50 mb AGL average.

was 564 and 266 $m^2 s^{-2}$, respectively. The Energy Helicity Index (EHI, Hart and Korotky 1991) for the 0-3 and 0-1 km layers was 14.3 and 6.1, respectively. Along with showing that EHI has value in discriminating between tornadic supercell and non-tornadic environments, Rasmussen and Blanchard (1998) showed that the EHIs of 1.5 or greater were present in half of their tornado soundings. The comparative EHI values for this day should be considered as very large. Consistent with the small dew point depressions in the surface observations, the lifted condensation level was just 555 m. Rasmussen and Blanchard (1998) have shown that low LCL heights are a favorable environmental factor on tornadic supercell days.

3. DATA COLLECTION AND METHODOLOGY

The mesonet on this day consisted of 3 field teams with nowcasting support from the University of Northern Colorado. The instrumentation and driving software was nearly identical on all vehicles. The type of instrumentation and mobile mesonet station configuration is similar to that presented by Straka et al. (1996). More recent models of the instrumentation were used when available. Field procedures were developed such that the GPS could be used for vehicle direction at all times eliminating the need for a flux gate compass. Data was recorded from the mesonet stations every 2 s. Twelve second averaged data was used in most of the mesonet analysis. The mesonet dataset was bias checked/adjusted and quality controlled in a manner consistent with Markowski et al. (2002). Given the lack of nearby ASOS stations and mesoscale nature of the environment north of the warm front, a base state to assess perturbation quantities of thermodynamic variables was difficult to ascertain. We chose to use select times of mesonet data collection when the array was sampling air with a thermodynamic character deemed to be representative to the pre-storm environment.

The mesonet sampled 6 RFD/RFDBs in the locations depicted in Fig. 3 and with designations listed in Table 1. Of the 6 deployments, 4 were RFD surges. The remaining 2 samplings were of mature RFDs with no basis for which to trace to a specific surge time (if any). The mesonets were operationally spaced roughly 1 – 1.5 km apart to provide sufficient density to sample the gradients of interest. The Manchester storm produced far more RFD surge events than could be effectively sampled by the mesonet array (likely at least twice the number of RFD surge cycles sampled).

Table 1 RFD Events Sampled By Mesonet

Number	RFD Name	Event Type	Time Sampled
1	Cavour	surge	2347-2357
2	Iroquois	surge	0014-0019
3	Esmond	mature	0019-0028
4	Manchester	surge	0032-0056
5	Desmet	surge	0127-0138
6	Bryant	mature	0149-0200

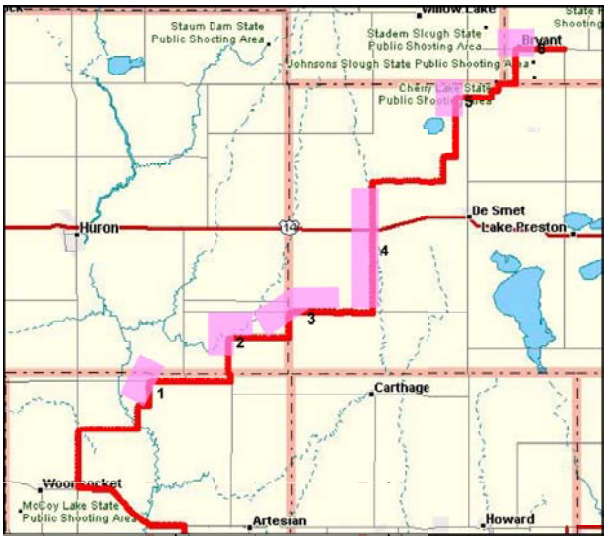

Fig. 3. Mesonet RFD event deployments on the Manchester supercell. Data was collected in RFD surges for events 1, 2, 4 and 5.

4. OBSERVATIONS AND ANALYSIS

Given the paucity of mobile mesonet datasets of multiple RFDs in cyclic supercells (especially within RFD surges when they can be identified), we wished to contrast the thermodynamic and kinematic character of the 4 RFD surges that were sampled for the Manchester storm. Figure 4 shows time series for the perturbation equivalent potential temperature (θ_e') and virtual potential temperature (θ_v'). Given the mesonet's distance from the closest WSR-88D location at Aberdeen (always over 120 km), and due to the lack of precipitation on the southern flank of the Manchester storm (only a few instances of light to moderate precipitation reaching the surface), the liquid water mixing ratio was neglected in the calculation of θ_v. The errors resulting from this omission when even moderate precipitation was occurring are only estimated to be a few tenths of

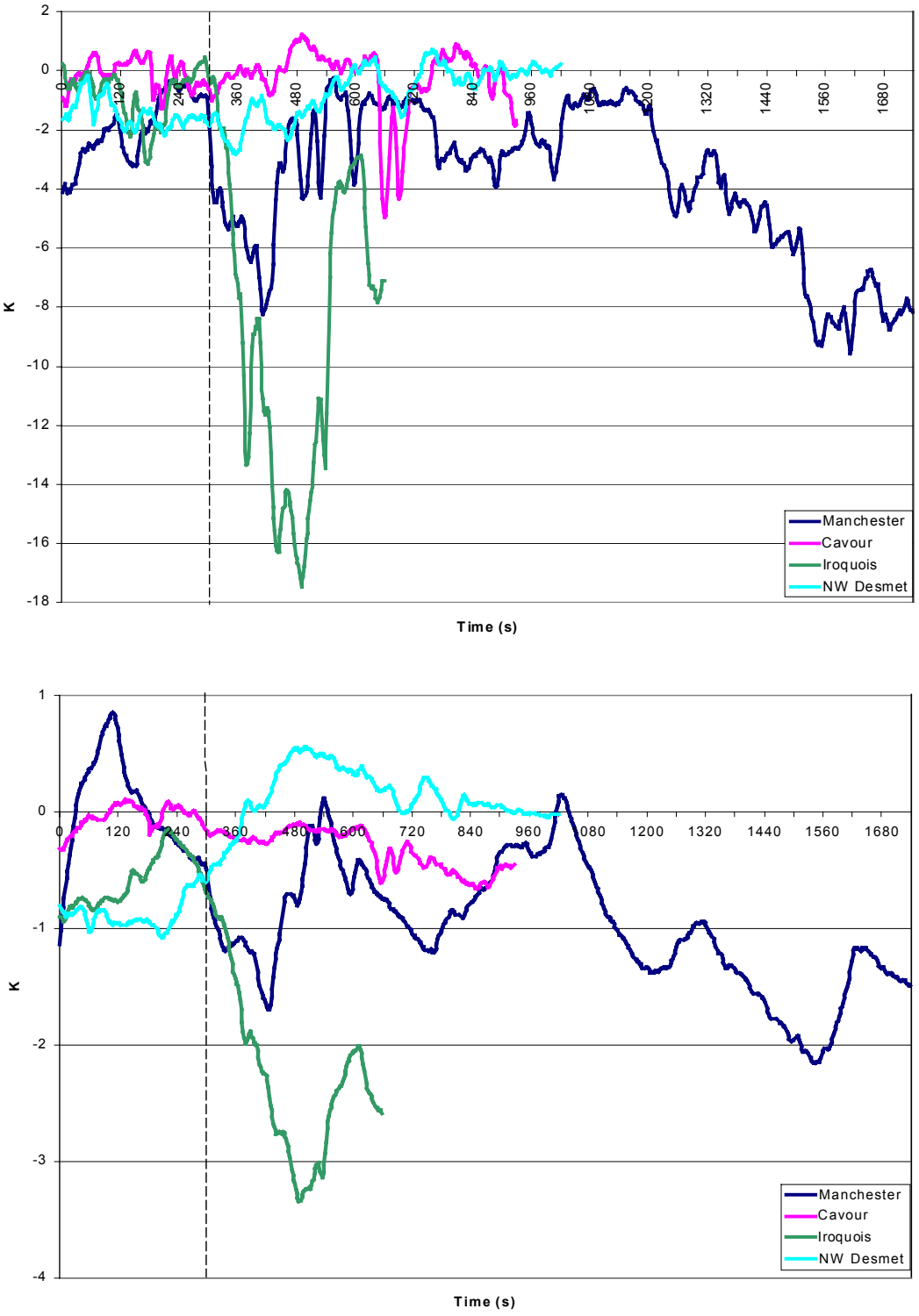

Fig. 4. θ_e' (top) and θ_v' (bottom) for the 4 RFD surges sampled. Data is from the lead vehicle (M1) that was positioned closest to the RFD surge core. The horizontal time line represents event-relative time. The dashed line delineates the point at which the RFD surge was entered with a 5 min trace leading up to this point.

one degree K. Evident in Fig. 4 are the wide variety of thermodynamic signals for RFD surge events within the same storm. In the case of the longer-duration Manchester RFD surge, there is significant observed thermodynamic variability due to the evolution of the surge and due to the location within the surge the array was sampling. Fig. 5 has been created to provide a visual perspective of the 4 RFD surge events. The Cavour RFD surge was the second known surge for the Manchester supercell. The first surge and tornado (F3) occurred earlier near Woonsocket at approximately 2320 UTC. The Cavour surge could be designated as qualitatively "warm" with only very small θ_e' and θ_v' values (< 1 K deficits) for the majority of the sampling period. Yet, even with a well defined RFD surge notch and very rapid rotation observed with the wall cloud (see Fig. 5a), tornadogenesis did not occur. Perhaps the failure was due to insufficient kinematics present at low-levels. Although within 1-2 km of the wall cloud centroid and definitively penetrating the RFD surge, the peak 3 m wind speed measured by the lead team was only 26 kt.

The next RFD surge cycle occurred approximately 15 min later, and could be considered strikingly cold by comparison with peak θ_e' deficits exceeding 17 K, although θ_v' deficits only peaked just above 3 K. It was remarkable that the same supercell in two adjacent RFD cycles produced such contrasting thermodynamic signals. This cycle was a case of tornadogenesis failure as might be expected based on the results of Markowski et al. (2002). The visual manifestation of this RFD surge cycle was a well defined notch carving into the southwest side of the wall cloud as shown in Fig. 5b. Like the previous cycle, this event might be considered kinematically weak, with peak in-surge 3 m winds of 26 kts.

The third surge was associated with the Manchester tornado. This was a much longer event that lasted approximately 25 min. The thermodynamic time series are much more complex due to the mesonet sampling both the evolution of the RFD and differing portions of the RFD. Figure 6 is provided as a reference for perspective of the positions and select measurements of the mesonet relative to the storm and RFDB. As the edge of the Manchester RFD is initially penetrated, relatively cool conditions are experienced as shown in Fig. 4. This initial cooling in θ_e' and θ_v' is likely due to the mesonet experiencing residual outflow from a previous RFD cycle and due to a region along and just inside the RFDB of enhanced mixing that may be entraining the aforementioned outflow air into the leading edge region. As M1 moves into the undiluted RFD surge near the 480 s point in Fig. 4, the θ_e' and θ_v' deficits gradually become very small (at times ~ 1 K for θ_e' and ~0 K for θ_v') indicative of the RFD air being thermodynamically similar to the pre-storm environment. The M1 observations in the beginning portion of the first analysis period in Fig. 6 reflect these "warm" thermodynamic conditions in the core of the RFD surge. Near the time of minimum θ_e' and θ_v', on the southern periphery of the tornadic region, a well-defined RFD notch had developed. Note this notch evolution in the wide angle perspective images shown in Figs 5c and 5d. At this point, the lead vehicle was approximately 1 km from the tornado with an audible roar. Unlike the previous 2 RFD surge cycles, this cycle was kinematically strong with M1 and M3 recording 49 kt and 57 kt peak gusts near this time (~0036 UTC), respectively (see Fig. 6). For safety reasons, the mesonet array temporarily stopped, only to resume pursuit in 3 min. As the undilute portion of the RFD surge pulls away from M1, a drop in θ_v' may be immediately seen with a slower response realized for θ_e'. As M1 once again catches the undilute portion of the RFD (0044 UTC), the θ_e' and θ_v' deficits shrink to their previous levels. At this point in time, the tornado had just passed through Manchester (Fig. 5e). Once again, with the lead team within 1 - 1.5 km of the very large tornado, the pursuit was temporarily halted. The same pattern repeats in the θ_e' and θ_v' time series; however, upon re-established sampling of the intense part of the RFD, the trend was for larger θ_e' and θ_v' deficits until tornado demise at 0057 UTC. The cooling trend of the RFD appeared to coincide with precipitation that was first observed south of the tornadic area at 0043 UTC (Fig. 6). Up to this time, even at distances approaching approximately 1 km from the tornado, no precipitation was observed by the mesonet. Perhaps more or larger hydrometeors were now populating a growing hook structure (from a radar reflectivity perspective) at this point in the storm's evolution. Evaporative cooling was a likely contributor to the cooling trend of the RFD. This trend directly coincided with the tornado diameter shrinking and ultimately dissipating.

One noteworthy aspect of the mesonet RFD observations was the very small-scale nature of what might be considered that part of the RFD that could be described as the undilute surge. The lead mesonet team had to get within about 1.5 km of the tornado to really sample with some confidence the RFD core. The results plotted in

Fig. 5. Visual perspective from the M1 lead vehicle of RFD surge events: a) Cavour (2355 UTC), b) Iroquois (0016 UTC), c) Manchester (0032 UTC), d) Manchester (0037 UTC), e) Manchester (0043 UTC, tornado just north of town), and f) Desmet (0130 UTC). All images shown (except image **e**) reflect wide angle settings to reveal the maximum in storm structure at close range and are looking north to north-northwest. (All images © B. Lee and M. Grzych)

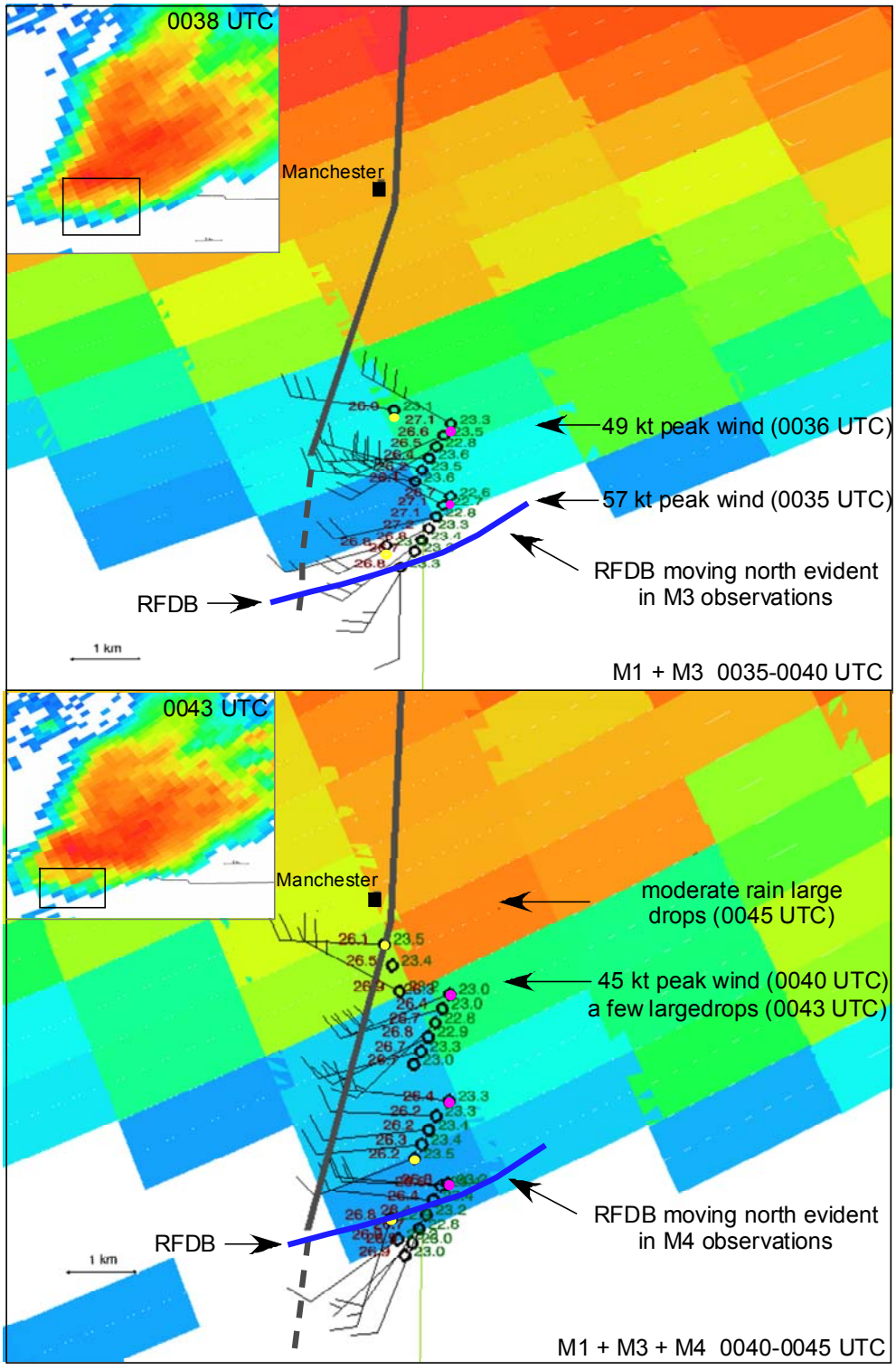

Fig. 6. Time space converted mesonet data for M1+M3 centered on 0038 UTC (top) and for M1+M3+M4 centered on 0043 UTC (bottom). The inset image at the upper left shows the storm-relative region of interest. The bold gray line is the tornado centroid track verified by the ANSWERS damage survey. Note that the tornado was much wider (~1 km max. width) than the tracking line over much of its life. The dashed line represents the early tornado track based on multi-team videography. Specific mesonet data points are separated by 30 s with some points removed for clarity. The data represents 12 s averaged observations for wind (kts), fast temperature (C, upper left) and dew point (C, upper right). The magenta (yellow) station circle represent the first (last) observation of a team. Peak instantaneous winds are noted.

Fig. 4 lend credence to this assumption of scale. For another tornadic supercell deployment on 9 June 2003 near Bassett, Nebraska, the ANSWERS mesonet, operating in close range to a developing tornado, observed similarly very small-scale character to the RFD surge that appeared to be associated with tornadogenesis (see P11.3). As indicated in Fig. 6, the changes in wind speed and direction over just 1-2 km is very considerable.

One other aspect of the mesonet observations appears to support the idea of the RFD for the Manchester cycle (and likely in other events with significant tornadoes) being fundamentally different thermodynamically than most outflows from thunderstorms. Typical thunderstorm outflows are density currents, generally moving away from their source region from a ground-relative perspective (Charba 1974; Wakimoto 1982; Droegemeier and Wilhelmson 1987). To a certain extent, their motion depends both upon their density difference with the ambient environment and the flow-force balance at the outflow leading edge as the current interacts with the environment. The RFDB during the Manchester cycle, even with only a weak opposing southerly wind component in the ambient environment, did not have any southerly propagation. In fact, the boundary motion had a northerly component, essentially pulling north consistent with the storm's northerly propagation component. This may be seen in the M3 observations for the 0035-0040 UTC analysis period and the M4 observations for the 0040-0045 UTC analysis period in Fig. 6. Due to the mesonet deployment along a north-south road, only the RFDB's north-south propagation component could be determined.

There were several RFD surge events after the Manchester tornado, but due to ANSWERS teams temporarily disengaging from the storm to participate in search and rescue activities in the F4 damage path just north of Manchester, the project was not able to get into position for another successful RFD surge deployment until 0127 UTC. This RFD surge was associated with one or more tornadoes northwest of Desmet. A wide angle perspective of one of these tornadoes is shown in Fig. 5f as data was being taken by the array. From a thermodynamic perspective, as shown in Fig. 4, this was one of the warmest RFD surges measured with θ_v values slightly exceeding that of the storm inflow and θ_e' deficits generally less than 2 K. Similar to the Manchester RFD surge, this surge was kinematically strong with a peak wind of 44 kts reported by M1 within the undiluted surge core. While this surge was similar to the Manchester surge cycle in kinematic intensity, thermodynamic character (actually warmer than the Manchester surge), and tornadogenesis success, the character of the resultant tornado was very different. The primary tornado associated with this RFD surge had a life span of about 5 min and was of F1 intensity.

5. DISCUSSION

The thermodynamic and kinematic analysis of the multiple RFD surge events for the Manchester supercell demonstrates the wide variations possible in RFD surges from a common parent cell. Comprehensive explanations for these differences in RFD character will likely be the focus of research for a considerable number of years. The cases analyzed support the conclusions of Markowski et al. (2002) concerning the increased likelihood of tornadogenesis accompanying mild/warm RFDs. If a mild/warm RFD surge is considered a necessary condition for tornadogenesis (especially significant tornadoes), the analysis of the Manchester supercell RFD surges demonstrate the insufficiency of this condition (the insufficiency of this condition was also noted in Markowski et al.)

The project was fortunate to capture a large portion of the RFD surge evolution associated with the F4 Manchester tornado. In this particular event, the RFD core remained "warm" with small θ_e' and θ_v' deficits (a thermodynamic signal nearly approaching the pre-storm environment) for at least an 11 min period (likely somewhat longer given deployment constraints). Thereafter, a gradual cooling ensued that was coincident with the appearance of light to moderate precipitation south of the tornado (large drops). Evaporative cooling was the probable reason for most of the cooling. The tornado contracted in diameter at the approximate same time the mesonet was observing the RFD cooling.

The RFD surges were found to be of small scale. During the Manchester tornado, the lead vehicle needed to be within about 1 – 2 km of the tornado to sample the undilute core of the RFD surge. Very large thermodynamic and kinematic horizontal gradients were found with these documented surge events. Although requiring further analysis, the mesonet data straddling the RFDB are suggestive of the presence of marked vertical vortex sheets residing along the boundary.

A final notable aspect of the RFDB associated with the Manchester surge involved its propagation. Unlike most outflows boundaries that propagate away from their ground-relative source region (in the absence of strong opposing

flow), the RFDB associated with this surge actually propagated in a northerly direction during the Manchester tornado. With only a weak southerly wind component in the ambient environment, a typical density driven outflow boundary would have demonstrated a southerly motion component. That the RFDB in this case had no southerly motion component attests to its thermodynamic character being not dissimilar to the ambient air outside of the RFD surge. In this case, the propagation might be construed as a momemtum surge rather than being driven by density gradients.

6. ACKNOWLEDGEMENTS

This research was supported by the National Science Foundation under grants ATM-0105279 and ATM-0432408. The authors thank all Project ANSWERS 2003 participants for their contributions. Erik Crosman and Brian Guarente are recognized for their considerable efforts in managing software development and operational portions of the project. Matt Grzych is acknowledged for his contributions in the construction of the UNC mesonets. Mesonet data plotting and analysis was greatly facilitated through the use of MAP software developed by Erik Rasmussen.

7. REFERENCES

Charba, J., 1974: Application of a gravity current model to analysis of a squall line gust front. *Mon. Wea. Rev*., **102**, 140-156.

Davies-Jones, R. P., D.W. Burgess, and M. Foster, 1990: Test of helicity as a forecast parameter. Preprints, *16th Conf. on Severe Local Storms*, Kananaskis Park, AB, Canada, Amer. Meteor. Soc. 588-592.

Droegemeier, K. K., and R. B. Wilhelmson, 1987: Numerical simulation of thunderstrom outflow dynamics. Part I: Outflow sensitivity experiments and turbulence dynamics. *J. Atmos. Sci.*, **44**, 1180-1210.

Hart, J. A., and W. Korotky, 1991: The SHARP workstation v1.50 users guide. National Weather Service, NOAA, US. Dept. of Commerce, 30 pp. [Available from NWS Eastern Region Headquarters, 630 Johnson Ave., Bohemia, NW 11716.]

Markowski, P. M., J. M. Straka, and E. N. Rasmussen, 2002: Direct surface thermodynamic observations within the rear-flank downdrafts of nontornadic and tornadic supercells. *Mon. Wea. Rev.,* **130**, 1692-1721.

Rasmussen, E. N., and D. O. Blanchard, 1998: A baseline climatology of sounding-derived supercell and tornado forecast parameters. *Wea. Forecasting*, **13**, 1148-1164.

Straka, J. M., E. N. Rasmussen, and S. E. Fredrickson, 1996: A mobile mesonet for fine-scale meteorological observations. *J. Atmos. Oceanic Technol*., **13**, 921-936.

Wakimoto, R. M., 1982: The life cycle of thunderstorm gust fronts as viewed with Doppler radar and rawinsonde data. *Mon. Wea. Rev.*, **110**, 1060-1082.